L-DOPA Neurotoxicity Is Mediated by Up-Regulation of DMT1−IRE Expression

Fang Du[1], Zhong-ming Qian[2,3]*, Li Zhu[2,3], Xiao Mei Wu[1], Wing-ho Yung[1], Ting-yuk Tsim[1], Ya Ke[1]*

1 Department of Physiology, Faculty of Medicine, The Chinese University of Hong Kong, New Territories, Hong Kong, 2 Department of Applied Biology & Chemical Technology, Hong Kong Polytechnic University, Kowloon, Hong Kong, 3 Department of Neurobiology and Jiangsu Key Laboratory of Neuroregeneration, Nantong University, Nantong, People's Republic of China

Abstract

Background: The mechanisms underlying neurotoxicity caused by L-DOPA are not yet completely known. Based on recent findings, we speculated that the increased expression of divalent metal transporter 1 without iron-response element (DMT1−IRE) induced by L-DOPA might play a critical role in the development of L-DOPA neurotoxicity. To test this hypothesis, we investigated the effects of astrocyte-conditioned medium (ACM) and siRNA DMT-IRE on L-DOPA neurotoxicity in cortical neurons.

Methods and Findings: We demonstrated that neurons treated with L-DOPA have a significant dose-dependent decrease in neuronal viability (MTT Assay) and increase in iron content (using a graphite furnace atomic absorption spectrophotometer), DMT1−IRE expression (Western blot analysis) and ferrous iron (55Fe(II)) uptake. Neurons incubated in ACM with or without L-DOPA had no significant differences in their morphology, Hoechst-33342 staining or viability. Also, ACM significantly inhibited the effects of L-DOPA on neuronal iron content as well as DMT1−IRE expression. In addition, we demonstrated that infection of neurons with siRNA DMT-IRE led to a significant decrease in DMT1−IRE expression as well as L-DOPA neurotoxicity.

Conclusion: The up-regulation of DMT1−IRE and the increase in DMT1−IRE-mediated iron influx play a key role in L-DOPA neurotoxicity in cortical neurons.

Introduction

Parkinson's disease (PD) is a progressive neurodegenerative disorder that affects approximately 1% of the people over the age of 60 [1]. This disorder is mainly characterized by the degeneration of dopamine-containing neurons in the substantia nigra. This brain section is therefore deprived of adequate amounts of the neurotransmitter dopamine [2]. Because dopamine is unable to access the brain directly, L-3,4-dihydroxyphenylala-nine (L-DOPA), its natural precursor, is used in clinical treatment of patients with PD. Until now, L-DOPA remains the most effective drug for the symptomatic control of PD [3,4]. However, accumulated evidence shows that the therapeutic efficacy of L-DOPA is gradually lost over time, and abnormal involuntary movements, dyskinesias, gradually emerge as a prominent side effect of the previously beneficial doses of the drug [5–7].

The precise molecular mechanisms underlying the neurotoxicity caused by L-DOPA are not yet completely known. Available data suggest that L-DOPA might have the ability to significantly affect iron distribution in the brain. The changes in brain iron distribution induced by L-DOPA might be one of the causes of the neurotoxicity of L-DOPA. A clinical study [8] demonstrated that L-DOPA could significantly affect brain ceruloplasmin (CP), a major factor in the regulation of regional brain iron, and that L-DOPA-treated PD patients had a significantly higher CP than those who were not given L-DOPA. A pathological study of postmortem brain tissue showed that the levels of iron storage protein ferritin were significantly lower in several brain regions of PD patients treated with L-DOPA than those in the age-matched control patients [9]. In a recent study, we demonstrated that L-DOPA induces a significant increase in the expression of divalent metal transporter 1 without iron-response element (DMT1−IRE), but not divalent metal transporter 1 with iron-response element (DMT1+IRE), TfR1 or Fpn1, and a remarkable increase in ferrous uptake in cells [10].

Based on these findings, plus the potential role of DMT1−IRE in neuronal iron uptake and the implication of iron as a major generator of reactive oxygen species, we speculated that the upregulation of DMT1−IRE might play a critical role in the development of L-DOPA neurotoxicity. L-DOPA might have a role to increase DMT1−IRE expression, which in turn leads to a remarkable increase in DMT1−IRE-mediated ferrous iron uptake

by neurons. Consequently, the increased ferrous iron in neurons generates highly reactive hydroxyl radicals via the Fenton reaction or Haber-Weiss reaction. In turn, these free radicals can damage the biological molecules of neurons, leading to the development of L-DOPA neurotoxicity. To test this hypothesis, we investigated the effects of astrocyte-conditioned medium (ACM) and siRNA DMT1−IRE on L-DOPA neurotoxicity by observing the changes in morphology and Hoechst 33342 staining, measuring neuronal viability, neuronal iron content, expression of DMT1−IRE, DMT1+IRE, TfR1 and Fpn1 proteins and ferrous iron uptake in cortical neurons in the present study. Our results provide solid evidence that the upregulation of DMT1−IRE plays a key role in the development of L-DOPA neurotoxicity in vitro. The findings imply that inhibition of DMT1−IRE expression or neuronal iron uptake might be an effective approach to prevent or delay the development of L-DOPA neurotoxicity in PD patients.

Materials and Methods

Materials

Unless otherwise stated, all chemicals were obtained from Sigma Chemical Company, St. Louis, MO, USA. The scintillation cocktail and tubes were purchased from Beckman Coulter Company, Fullerton, CA, USA and $^{55}FeCl_3$ from Perkinelmer Company, Wellesley, MA, USA. The antibodies against DMT1+IRE, DMT1−IRE and Fpn1 were purchased from Alpha Diagnostic International Company, San Antonio, TX, USA and mouse anti-rat TfR1 monoclonal antibody was obtained from BD Transduction Laboratories, BD Biosciences Pharmingen, USA. The specific antibodies against neuron microtubule-associated protein 2 (MAP2) and astrocyte glial fibrillary acadic protein (GFAP) were purchased from Chemicon International Ltd, UK and Hoechst 33342 from Polysciences Inc., Warrington, PA, USA.

Primary cortical neurons

Primary cortical neurons were prepared from embryonic Day 18 (E18) rats as previously described [11] with minor modifications. The purity of these cultures was assessed by staining for the neuron specific antibodies against MAP2 and the astrocyte marker GFAP.

Preparation of astrocytes culture medium

Primary astrocytes were prepared as previously described [12,13]. The purity of astrocyte cultures was determined using anti-GFAP antibody. The medium was changed to DMEM/F12 supplemented with 2% newborn calf serum (NCS), collected 48 hours later (astrocyte conditioned medium, ACM), centrifuged at 3000 r/min for 15 min to remove cellular debris and then stored at −80°C.

Experimental Design

To investigate the effects of L-DOPA on cortical neurons, the cells were treated with different concentrations of L-DOPA (0, 1, 5, 10, 100 or 200 μM) in DMEM+5%FBS for 16 hours and then morphological changes, neuronal viability, cell iron content, the expression of DMT1−IRE, DMT1+IRE, TfR1 and Fpn1 proteins and NTBI (non-transferrin bound iron) uptake were determined. To detect the effects of ACM on the neurotoxicity induced by L-DOPA, neurons were incubated with or without L-DOPA in DMEM+5%FBS or ACM for 16 hours followed by the relevant measurements. To further confirm whether the increased expression of DMT1−IRE was involved in the neurotoxicity induced by L-DOPA, neurons were pre-incubated with siRNA DMT1−IRE for 24 hours before treatment with L-DOPA.

Morphological observation

Morphological changes of the neurons were observed under phase contrast microscopy or fluorescence microscopy.

Determination of cell viability

The cell viability was determined using an MTT assay as described previously [14,15]. Optical density (OD) was measured at 570 nm by the use of the ELX-800 microplate assay reader (Bio-tek, USA).

Immunocytochemistry

Immunocytochemical experiments were performed using neuron specific mouse anti-MAP2, astrocyte specific anti-GFAP, rabbit anti-rat DMT1−IRE, DMT1+IRE, TfR1 and rabbit anti-mouse Fpn1 antibodies respectively [16]. Cortical neurons in slides were incubated with one of the above antibodies: anti-MAP2 (1:200), anti-GFAP (1:200), anti-rat DMT1−IRE (1:500), DMT1+IRE (1:500), TfR (1:200) and anti-mouse Fpn1 (1:500) for 24 hours, followed by FITC-labeled goat anti-mouse IgG (1:200), or Rhodamine-labeled goat anti-rabbit IgG (1:200) (Invitrogen, USA) as the secondary antibody. Fluorescent images were captured by using a Nikon Eclipse TE2000-U microscope (Nikon, UK) equipped with T-FL Epi-FI attachment and a SPOT cooled CCD camera (Diagnostic Instruments, INC, US). SPOT software version 4.6 was used for image acquisition (Diagnostic Instruments, INC, US).

Hoechst 33342 staining

Hoechst 33342 staining was used to detect morphological features of apoptotic cell death. Cortical neurons pre-treated with or without different concentrations of L-DOPA were stained with Hoechst 33342. The cells were then examined under a fluorescent microscope. Undamaged cell nuclei were large and diffusely stained whereas apoptotic nuclei showed chromatin that was condensed and fragmented.

Iron measurement

The slides were fixed with 4% paraformalin for 10 min. After three washes with PBS, the slides were incubated in Perl's solution containing 4% potassiumferrocanide and an equal volume of 1.2 mmol/L hydrochloride acid solution for 16 hours at 4°C and then washed with deionized water 3 times, followed by dehydration through 95% alcohol and mounting with xylene. Iron staining was observed under a Nikon Eclipse TE2000-U microscope (Nikon, UK). The total iron in the neurons was also determined using a graphite furnace atomic absorption spectrophotometer (GFAAS, Perkin Elmer, Analyst 100) as previously described [17,18].

Western blot analysis

Neurons that received different treatments were washed with ice-cold PBS, homogenized with lysis buffer and then subjected to sonication using Soniprep 150 (MSE Scientific Instruments, London, UK). After centrifugation at 10,000 g for 15 min at 4°C, the supernatant was collected, and protein content was determined using the Bradford assay kit (Bio-Rad). Aliquots of the cell extract containing 30 μg of protein were diluted in 2 μl sample buffer (50 mM Tris, pH 6.8, 2% SDS, 10% glycerol, 0.1% bromphenol blue, and 5% β-mercaptoethanol) and heated for 5 min at 95°C before SDS-PAGE on 10% gel and subsequently transferred to a pure nitrocellulose membrane. After the transfer, the membrane was blocked with 5% blocking reagent in Tris-buffered saline containing 0.1% Tween-20 overnight at 4°C. The membrane was rinsed in three changes of Tris-buffered saline/
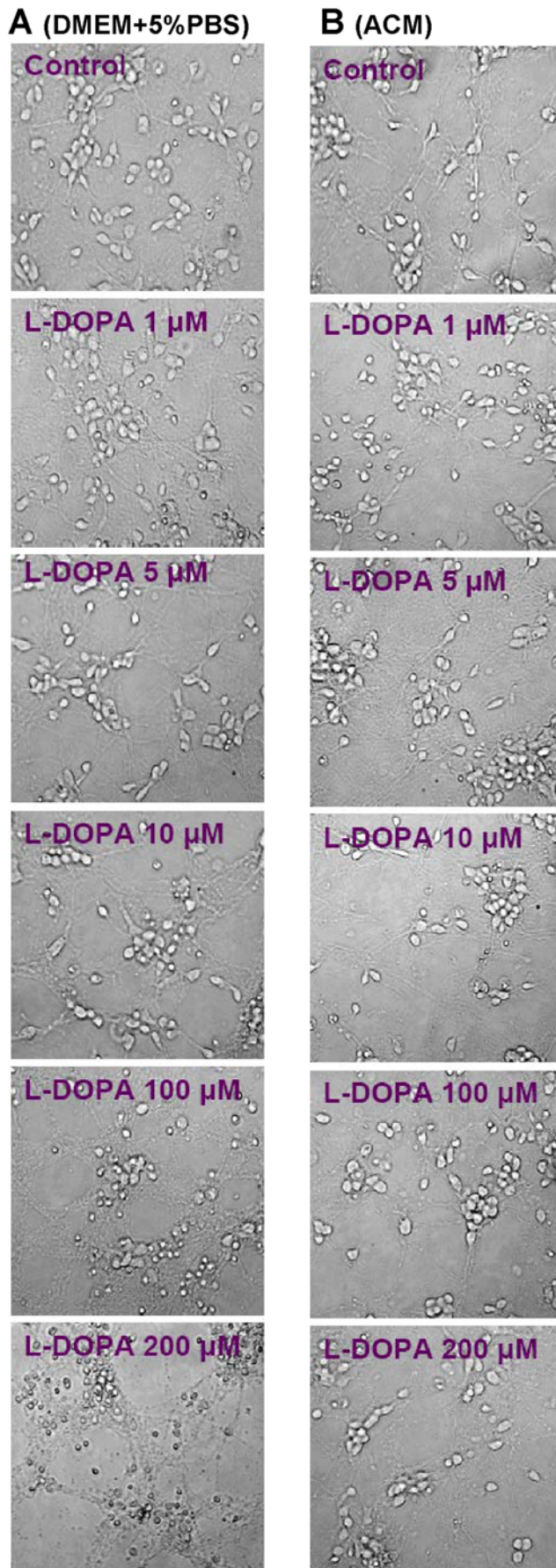
Figure 1. L–DOPA induced morphological changes in cortical neurons. Neurons were treated with L-DOPA (0, 1, 5, 10, 100, 200 µM) in DMEM+5%FBS (**A**) or astrocyte-conditioned medium (ACM) (**B**) for 16 hours and then morphological changes were observed as described in Materials and Methods.
doi:10.1371/journal.pone.0004593.g001

Tween-20, incubated in fresh washing buffer once for 15 min and twice for 5 min, and then incubated overnight at 4°C with primary antibodies: rabbit anti-rat DMT1+IRE, DMT1−IRE polyclonal antibodies, rabbit anti-mouse Fpn1 polyclonal antibody (1:5000); mouse anti-rat TfR1 monoclonal antibody (1:1000). After three washes, the blots were incubated with goat anti-rabbit or anti-mouse IRDye 800 CW secondary antibody (1:5000, Li-Cor) for 1 hour at room temperature. The intensity of the specific bands was detected and analyzed by Odyssey infrared imagine system (Li-Cor). To ensure even loading of the samples, the same membrane was probed with rabbit anti-rat β-actin polyclonal antibody at a 1:2000 dilution.

Construction of siRNA against DMT-IRE

pSUPER.retro vector (OligoEngine, USA) was used for expression of siRNA targeting on DMT1−IRE. The target sites for siRNA were designed by using an oligoEngine tool. The selected sequences were submitted to a BLAST search to avoid targeting the other human genome. Two 19-nucleotide sequences corresponding to nucleotides 1681–1699 and 1776–1794 of DMT1−IRE were selected to generate the pSUPER-hepcidin vectors. A control vector (pSUPER-Control) was constructed using a 19-nucleotide sequence (gcgcgctttgtaggattcg) with no significant homology to any mammalian gene sequence and therefore served as a non-silencing control (OligoEngine, USA). These sequences were inserted into the pSUPER.retro vector after digestion with BglII and HindIII and were transformed into BL21-A1 One ShotTM supercompetent cells (Invitrogen, USA). Several clones were obtained, and the vectors were amplified. Retroviruses expressing siRNA DMT1−IRE were produced by transfecting pSUPER-hepcidin vectors into amphotropic Phoenix packaging cell line according to the manufacturer's instructions. The obtained retrovirus was used to the in vitro infection of cells or in vivo injection of cerebroventricules.

Measurement of non-transferrin bound iron uptake

The radio-labelled 55Fe(II) (NTBI) solution was prepared and the Fe(II) uptake was measured as described previously [19]. Following pre-treatment with different concentrations of L-DOPA, the cells were washed with cold PBS and then incubated with or without 55Fe(II) for various periods of time. After being lysed, the cells were scraped off and transferred into Eppendorf tubes. A 50 µl aliquot was subjected to the detection of protein concentration. The cytosol was separated from the stromal fraction by centrifugation at 10,000 g for 20 min at 4°C using a Jouan centrifuge (DJB labcare Ltd., England). Scintillation solution (3 ml) was added to count the cpm. The total iron uptake was the sum of the cytosol and stromal fractions.

Statistical analysis

Statistical analyses were performed using SPSS software for Windows (version 10.0). Data were presented as mean±SEM. The difference between the means was determined by One-Way ANOVA followed by a Student-Newman-Keuls test for multiple comparisons. A probability value of $P<0.05$ was taken to be statistically significant.
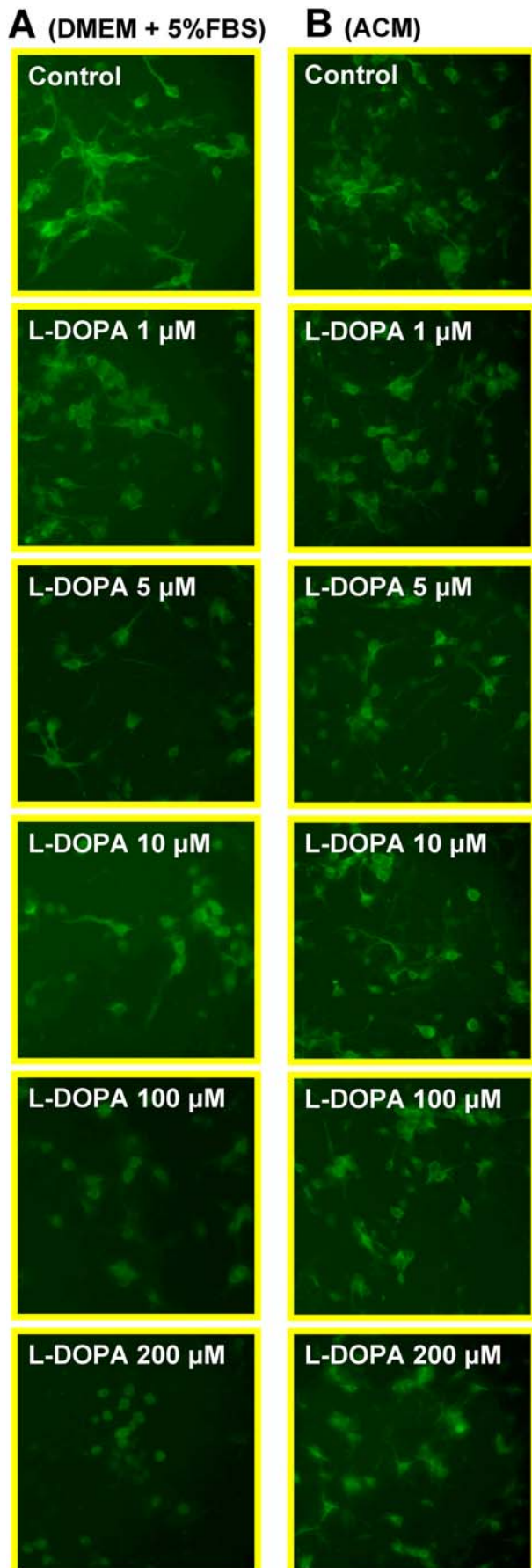
A (DMEM + 5%FBS)

Control

L-DOPA 1 μM

L-DOPA 5 μM

L-DOPA 10 μM

L-DOPA 100 μM

L-DOPA 200 μM

B (ACM)

Control

L-DOPA 1 μM

L-DOPA 5 μM

L-DOPA 10 μM

L-DOPA 100 μM

L-DOPA 200 μM

Figure 2. Immunocytochemistry of MAP2 in cortical neurons treated with or without L-DOPA. Neurons were exposed to L-DOPA (0, 1, 5, 10, 100, 200 μM) in DMEM+5%FBS (A) or astrocyte-conditioned medium (ACM) (**B**) for 16 hours and then immunostained for MAP-2 antibody as described in Materials and Methods.
doi:10.1371/journal.pone.0004593.g002

Results

Neurotoxicity induced by L-DOPA: morphological evidence and significantly decreased neuronal viability

Figure 1A presented the morphological observations in neurons treated with L-DOPA (0, 1, 5, 10, 100 or 200 μM) in DMEM+5%FBS for 16 hours. As compared to the controls, neurons pre-treated with L-DOPA displayed a dose-dependent morphological change. It was characterized by a progressive increase in the number of irregular cell bodies with disrupted and shrunken neuronal processes with the increase in the concentrations of L-DOPA in the medium. Pre-treatment with 200 μM of L-DOPA induced a significant reduction in or disappearance of the neuronal number or processes. The observations under phase contrast microscopy corresponded to the findings of immunostaining of cortical neurons for MAP2 (Figure 2A). Hoechst 33342 staining (Figure 3A) displayed a gradual increase in the number of condensed or fragmented nuclei (apoptosis) in cortical cells with the increase in the concentrations of L-DOPA. The number of condensed nuclei was the highest in the neurons pretreated with 200 μM of L-DOPA. The neuronal viability was determined using an MTT assay. As shown in Figure 4A, treatment of neurons with L-DOPA in DMEM+5%FBS for 16 hours led to a progressive decrease in the cell viability with the increase in the concentrations of L-DOPA. A significant decrease in viability was found in the neurons treated with 10, 100 or 200 μM of L-DOPA (P<0.01 or 0.001).

ACM diminishes L-DOPA-induced neurotoxicity

Treatment with L-DOPA did not induce any significant changes in neuronal morphology or the immunostaining of cortical neurons for MAP2 when the incubation medium DMEM+5%FBS was replaced by ACM. No significant differences in cell morphology (Figure 1B) or the MAP2 (Figure 2B) were found among the neurons treated with or without different concentrations of L-DOPA. Consistent with this observation, Hoechst 33342 staining demonstrated that cell nuclei remained unchanged in neurons that were incubated with 200 μM of L-DOPA in ACM (Figure 3B). No significant differences in Hoechst 33342 staining were found between the neurons treated with or without 200 μM of L-DOPA in ACM. Furthermore, cell viabilities in the neurons that were incubated with 10, 100 or 200 μM of L-DOPA in ACM were significantly higher than those in the neurons incubated with same concentrations of L-DOPA in DMEM+5%FBS medium (P<0.001 or 0.0001) (Figure 4B).

L-DOPA induces a significant increase in iron content in cortical neurons

Figure 5A presented the data on iron stain in neurons that were treated with different concentrations of L-DOPA in DMEM+5%FBS for 16 hours. The control neurons had large cell bodies and more elaborate processes with a tiny amount of iron located primarily in the cell bodies. No changes in iron distribution and morphology were found in neurons pre-treated with 1 μM of L-DOPA. In the neurons treated with 5 μM of L-DOPA, iron content in the cell body appeared to have increased but the body shape and body size remained the same. A significant
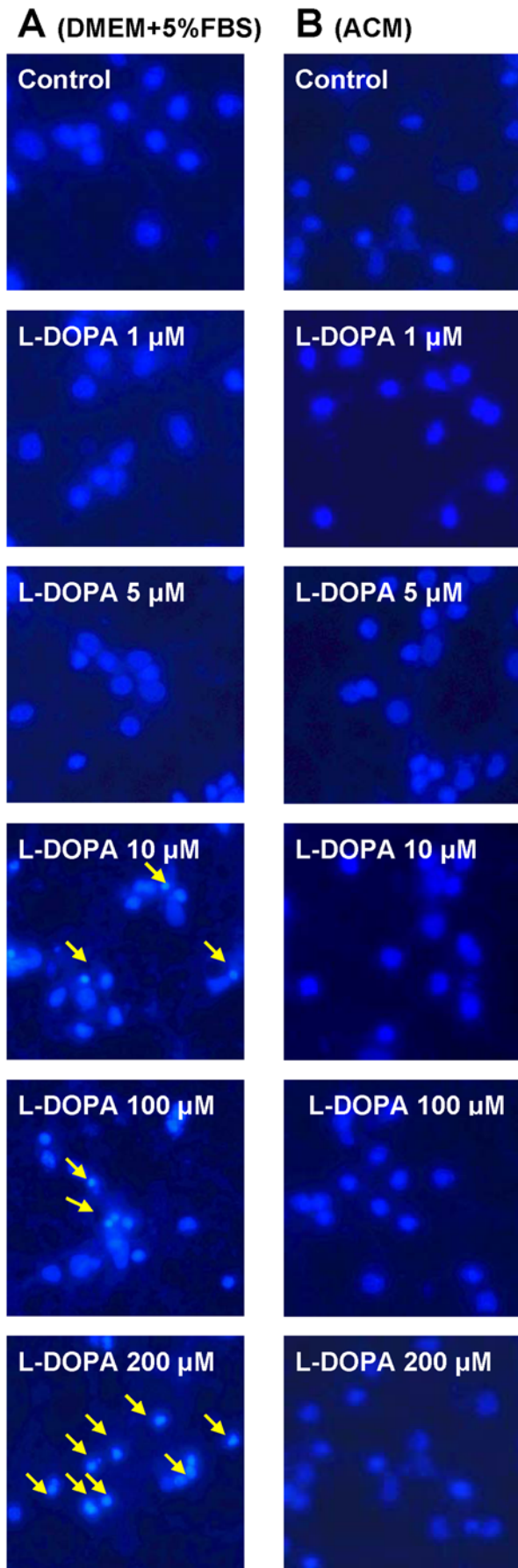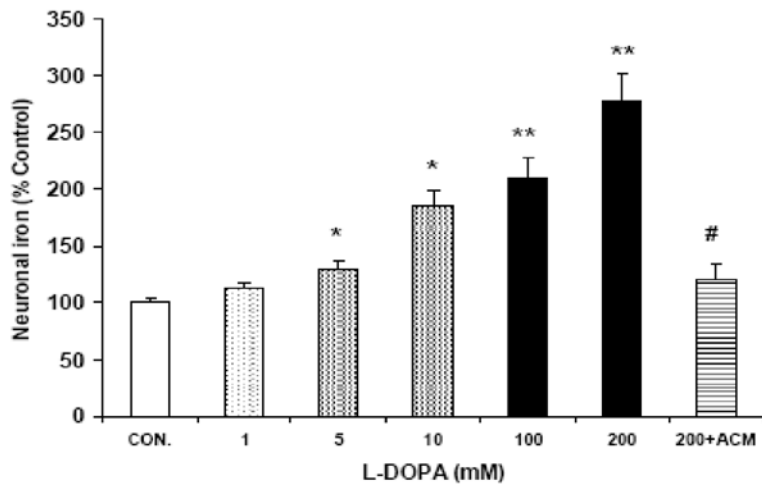
A (DMEM+5%FBS)
Control
L-DOPA 1 µM
L-DOPA 5 µM
L-DOPA 10 µM
L-DOPA 100 µM
L-DOPA 200 µM

B (ACM)
Control
L-DOPA 1 µM
L-DOPA 5 µM
L-DOPA 10 µM
L-DOPA 100 uM
L-DOPA 200 µM

Figure 3. Hoechst 33342 staining in cortical neurons treated with or without L-DOPA. Neurons were exposed to 0, 1, 5, 10, 100 or 200 µM of L-DOPA in DMEM+5%FBS (**A**) or 0 or 200 µM of L-DOPA in astrocyte-conditioned medium (ACM) (**B**) for 16 hours and then Hoechst 33342 staining was performed. The nuclei with fluorescing intensely, shrunken in size and irregular in shape are indicated in arrows. doi:10.1371/journal.pone.0004593.g003

increase in iron density and positive iron staining in the processes was observed in the neurons treated with 10, 100 or 200 µM of L-DOPA. The iron accumulation was most pronounced in neurons pre-treated with 200 µM of L-DOPA, which appeared dystrophic with large and irregularly-shaped cell bodies attaching to densely beaded processes and the iron filling the cell body and processes completely. The measurement of total iron provided quantitative evidence for the ability of L-DOPA to induce a significant increase in neuronal iron contents. The total iron was significantly higher in neurons pretreated with 5, 10, 100 or 200 µM of L-DOPA than in the controls (Figure 5C).

ACM reduces iron content in cortical neuron treated with L-DOPA

Figure 5B presented the data on iron stain in neurons that were treated with different concentrations of L-DOPA in ACM. No significant changes in neuron iron contents were observed when
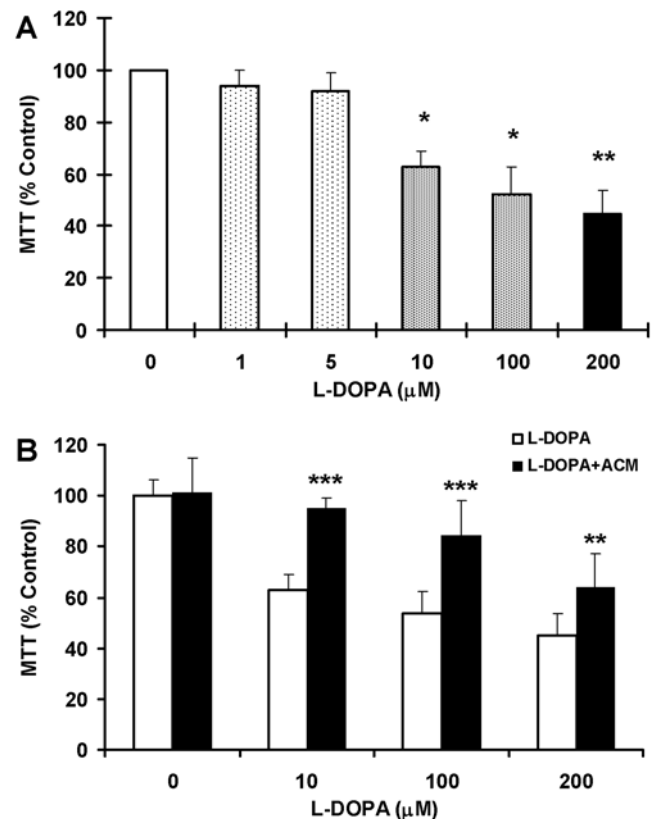
Figure 4. Effects of L-DOPA on neuronal viability. Neurons were treated with 0, 1, 5, 10, 100 or 200 µM of L-DOPA in DMEM+5%FBS for 16 hours (**A**) or incubated with 0, 10, 100 or 200 µM of L-DOPA in DMEM +5%FBS medium (L-DOPA) or astrocyte-conditioned medium (L-DOPA+ACM) for 16 hours (**B**). The neuronal viability was then determined using an MTT assay. Data are the mean±SEM (percentage of control) of three independent experiments performed in triplicate. **A**: *P<0.01, **P<0.001, vs. the control (0 µM). **B**: **P<0.001, ***P<0.0001 vs. the corresponding controls. doi:10.1371/journal.pone.0004593.g004

A (DMEM+5%FBS)

Con.   L-DOPA 1 µM   L-DOPA 5 µM

L-DOPA 10 µM   L-DOPA 100 µM   L-DOPA 200 µM

B (ACM)

Con.   L-DOPA 1 µM   L-DOPA 5 µM

L-DOPA 10 µM   L-DOPA 100 µM   L-DOPA 200 µM

C (total iron in neurons)

neurons were incubated in ACM with L-DOPA (0, 1, 5, 10, 100 or 200 µM) for 16 hours (Figures 5B). Treatment with ACM induced a significant decrease in iron content in cortical neurons treated

with 200 µM of L-DOPA (Figure 5C). These results demonstrated that ACM has the ability to inhibit the effect of L-DOPA on iron content in cortical neurons.
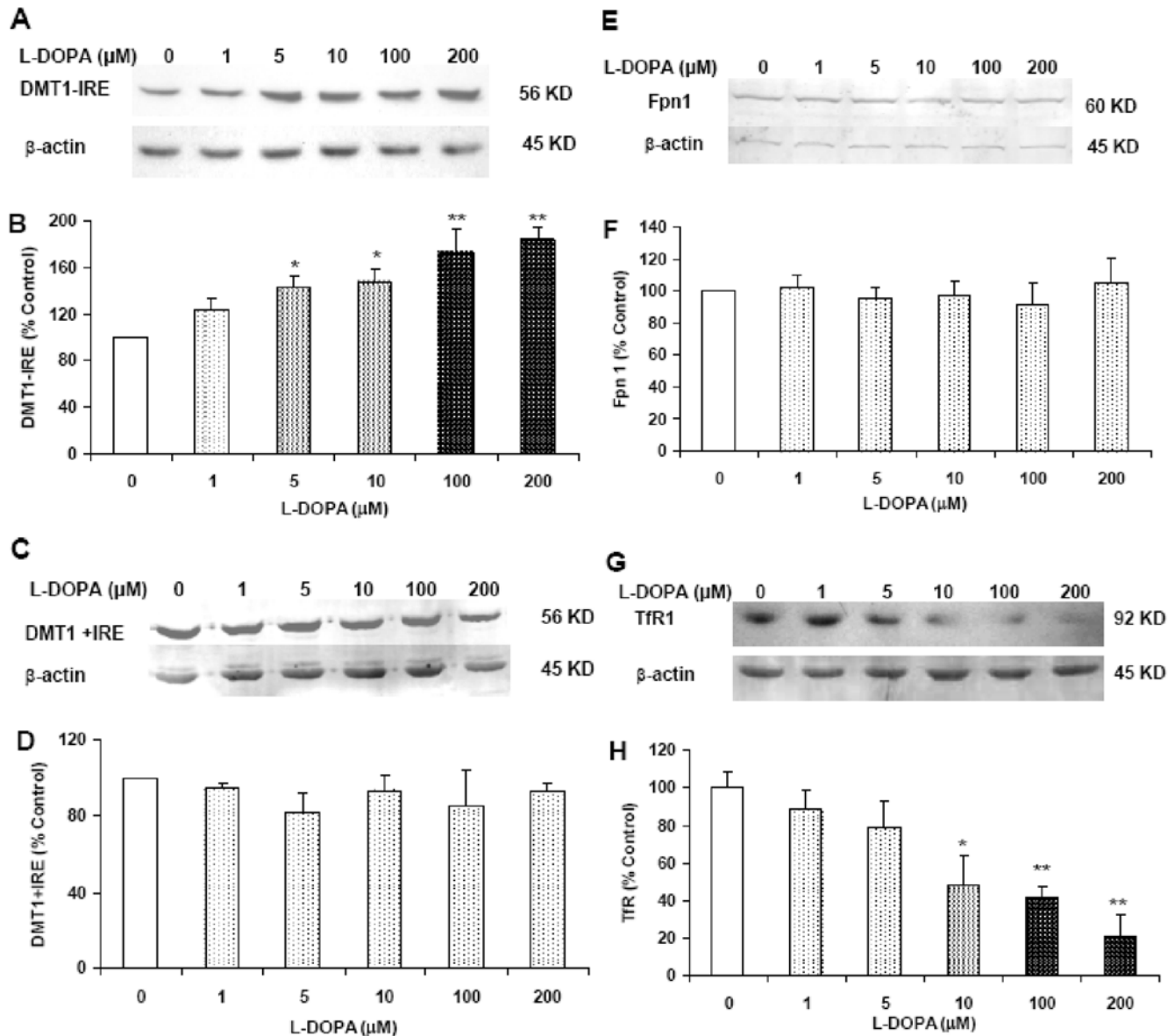
Figure 6. Effects of L-DOPA on the expression of DMT1−IRE, DMT1+IRE, Fpn1 and TfR1 proteins in cortical neurons. Neurons were treated with L-DOPA (0, 1, 5, 10, 100, 200 µM) in DMEM+5%FBS for 16 hours and the expression of proteins was determined using Western blot analysis. **A**, representative Western blots of DMT1−IRE and β-actin. **B**, the relative values of DMT1−IRE protein expression. **C**, representative Western blots of DMT1+IRE and β-actin. **D**, the relative values of DMT1+IRE protein expression. **E**, representative Western blots of Fpn1 and β-actin. **F**, the relative values of Fpn1 protein expression. **G**, representative Western blots of TfR1 and β-actin. **H**, the relative values of TfR1 protein expression. Data are means±SEM (percentage of control) of four independent experiments. L-DOPA treatment induced a dose-dependent decrease in TfR. There were no significant differences in the levels of DMT1+IRE and Fpn1 protein between neurons treated with and without L-DOPA. * P<0.05, ** P<0.01 vs. the control.
doi:10.1371/journal.pone.0004593.g006

?

Figure 9. Effects of astrocyte-conditioned medium on the expression of DMT1−IRE, DMT1+IRE, Fpn1 and TfR1 proteins in cortical neurons treated with L-DOPA. Neurons were treated with L-DOPA (0, 100 or 200 μM) in ACM for 16 hours and Western blot analysis was then conducted. **A**, representative Western blots of DMT1−IRE and β-actin. **B**, the relative values of DMT1−IRE protein expression. **C**, representative Western blots of DMT1+IRE and β-actin. **D**, the relative values of DMT1+IRE protein expression. **E**, representative Western blots of Fpn1 and β-actin. **F**, the relative values of Fpn1 protein expression. **G**, representative Western blots of TfR1 and β-actin. **H**, the relative values of TfR1 protein expression.

Figure 10. Effects of siRNA DMT−IRE on DMT1−IRE expression and L-DOPA-induced neurontoxicity in cortical neurons. A and **B**: Neurons were pre-incubated with siRNA DMT−IRE for 24 hours and Western blots analysis was then performed (**A**: representative Western blots of DMT1−IRE and β-actin, and **B**: the relative values of DMT1−IRE protein in neurons infected with or without siRNA DMT−IRE). Data are means±SEM (percentage of control) of four independent experiments performed in triplicate. **P<0.01 vs. the control. **C**: Neurons were pre-incubated with siRNA DMT−IRE for 24 hours and then treated with different concentrations of L-DOPA (0, 1, 5, 10, 100, 200 μM) in DMEM+5%FBS medium fro 16 hours. The neuronal viability was then determined using an MTT assay. Data are the mean±SEM (percentage of control) of four independent experiments performed in triplicate. *P<0.05, ***P<0.001 vs. the corresponding controls.
doi:10.1371/journal.pone.0004593.g010

the well-known function of iron in the generation of reactive oxygen species, we hypothesized that the upregulation of DMT1−IRE might play a critical role in the development of L-DOPA neurotoxicity. In the present study, efforts were made to test this hypothesis. Based on several lines of solid evidence obtained from this study, we concluded that the L-DOPA-induced neurotoxicity is mediated by the upregulation of DMT1−IRE expression in cortical neurons.

The first evidence comes from the investigation of the effects of L-DOPA on cortical neurons. Our data clearly demonstrated that treating neurons with different concentrations of L-DOPA induces not only a significant change in morphology or Hoechst-33342 staining but also a dose-dependent decrease in neuronal viability, confirming that L-DOPA can induce neurotoxicity in ou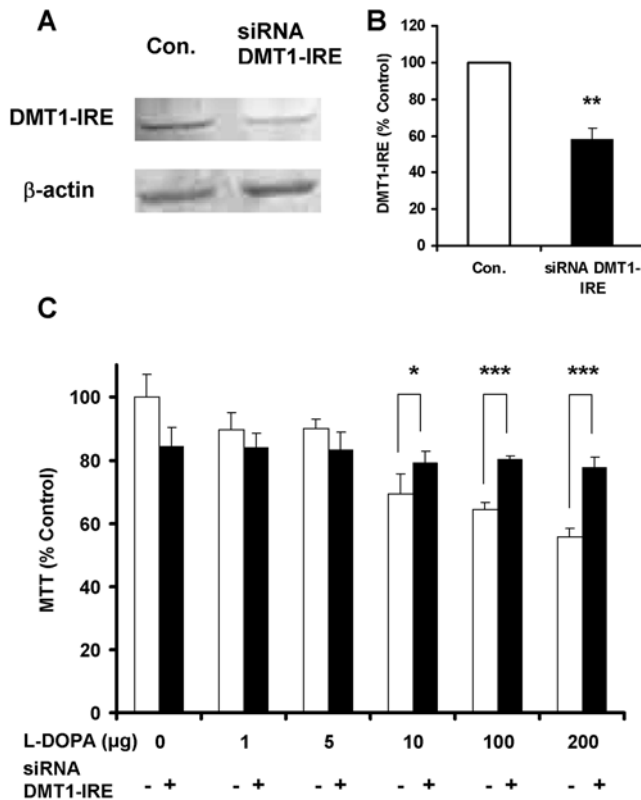r experimental conditions. Meanwhile, the treatment also resulted in a significant dose-dependent increase in iron content, ferrous iron

uptake and DMT1−IRE protein expression in cortical neurons. Furthermore, correlation analysis showed that the expression of DMT1−IRE protein is significantly correlated with 55Fe uptake (positively) and neuronal viability (negatively) in cortical neurons treated with different concentrations of L-DOPA; respectively. These findings support a role of L-DOPA in the increased DMT1−IRE expression as well as in the connection of the increased DMT1−IRE with the increased neuron iron content. In addition, both western blot and immunocytochemistry analysis showed that L-DOPA didn't induce any changes in the expression of DMT1+IRE or Fpn1. A significant decrease in TfR1 expression, rather than an increase, was found in the neurons treated with L-DOPA. These results showed that the increase in neuronal iron content induced by L-DOPA is due to neither the decrease in Fpn1-mediated iron efflux nor the increase in DMT1+IRE or TfR1-mediated iron uptake. On the other hand, these results also provided further support that L-DOPA has a role to increase DMT1−IRE expression and that the increased iron content in neurons induced by L-DOPA results from the increased DMT1−IRE-mediated iron uptake.

The second evidence is obtained from the study on the effects of ACM on L-DOPA-induced neurotoxicity. It has been reported that astrocytes have a role in the reduction of neuronal cell death following a variety of cellular stresses, such as excitotoxicity and oxidative stress [23–25]. Also, it has been demonstrated that glia conditioned medium (GCM) protects fetal rat midbrain neurons in culture from L-DOPA toxicity [26]. We speculated that the neuroprotective role of GCM or ACM might be mediated by their ability to inhibit DMT1−IRE expression as well as iron accumulation in neurons. Therefore, we investigated the effects of ACM on morphology, Hoechst 33342 staining, viability, neuron iron content and DMT1−IRE expression in the neurons treated with L-DOPA by incubating neurons in ACM with or without different concentrations of L-DOPA for 16 hours. The results obtained on the morphology, Hoechst 33342 staining and neuronal viability clearly demonstrated that ACM significantly diminishes L-DOPA-induced neurotoxicity. No significant differences were found in morphology, Hoechst-33342 staining and viability between the neurons incubated in ACM in the presence and those incubated in ACM in the absence of the same concentrations of L-DOPA. At the same time, western blot analysis and iron staining showed that ACM significantly reduces DMT1−IRE expression as well as neuron iron content. The similar tendencies of the effects of ACM on L-DOPA-induced neurotoxicity, DMT1−IRE expression and neuron iron content implied that ACM protects neurons from L-DOPA by its ability to inhibit DMT1−IRE expression and ferrous iron uptake.

The final piece of evidence is provided by the data on the effects of siRNA DMT−IRE on L-DOPA neurotoxicity. According to the findings on DMT1−IRE, L-DOPA neurotoxicity and the role of ACM, we expected that a decrease in DMT1−IRE expression should also be able to lead to a decrease in L-DOPA neurotoxicity. Therefore, we infected the cortical neurons with siRNA DMT−IRE to decrease DMT1−IRE expression to see whether L-DOPA neurotoxicity was hence changed in these neurons. As we expected, western blot analysis revealed a significant decrease in the expression of DMT1−IRE protein as well as iron content in the neurons infected with siRNA DMT−IRE. The MTT assay demonstrated that the viabilities in the neurons infected with siRNA DMT−IRE were significantly higher than those in the control neurons at all concentration points of L-DOPA we

examined. The findings showed that the decreased expression of DMT1−IRE induced by siRNA DMT−IRE can decrease neuronal iron accumulation and also L-DOPA neurotoxicity. These further confirmed that DMT1−IRE upregulation and the increased DMT1−IRE mediated iron influx play a key role in the development of L-DOPA neurotoxicity in primary neurons.

DMT1 (DCT1 or NRAMP2), a widely expressed membrane protein [27,28], is responsible for the uptake of a broad range of divalent metal ions [27–29]. There are four DMT1 isoforms that differ in their N- and C-termini arise from mRNA transcripts that vary both at their 5′-ends (starting in exon 1A or exon 1B) and at their 3′-ends giving rise to mRNAs containing (+) or lacking (−) the 3′-IRE [30]. The existence of DMT1 in the brain has been well determined [17,31]. The functions of DMT1+IRE and DMT1−IRE have not been completely understood [32]. However, available data support the notion that DMT1−IRE, rather than DMT1+IRE, is the entity responsible for the transmembrane transport of iron released from transferrin to the early endosomal lumen [10,22]. Recent studies also inferred that DMT1−IRE is predominantly found in three compartments: the plasma membrane, early/recycling endosomes, and the endoplasmic reticulum [22]. In the present study, we found that treatment of neurons with different concentrations of L-DOPA also resulted in a significantly dose-dependent increase in iron content, ferrous iron uptake and the expression of DMT1−IRE protein in cortical neurons. It was also found that there is a significant correlational relationship between the expression of DMT1−IRE protein and

55Fe uptake (positively) in cortical neurons treated with different concentrations of L-DOPA. These findings provide further support to the notion that DMT1−IRE, rather than DMT1+IRE, is the entity responsible for iron transmembrane transport as well as the role of DMT1−IRE upregulation in L-DOPA neurotoxicity.

In summary, in the present study we provided solid evidence for the first time for the association of DMT1−IRE with neurotoxicity induced by L-DOPA. We concluded that upregulation of DMT1−IRE and then the increased DMT1−IRE mediated iron influx play a critical role in L-DOPA neurotoxicity in primary cortical neurons. We also demonstrated for the first time that ACM's protection of cortical neurons from L-DOPA is at least partly due to its ability to inhibit DMT1−IRE expression and ferrous iron uptake and its antioxidative activity which might be due to the antioxidants supplied by astrocytes.

Author Contributions

Conceived and designed the experiments: ZMQ YK. Performed the experiments: FD LZ XMW WhY TyT. Analyzed the data: ZMQ YK. Contributed reagents/materials/analysis tools: WhY. Wrote the paper: ZMQ YK.

References

1. Jankovic J, Stacy M (2007) Medical management of levodopa-associated motor complications in patients with Parkinson's disease. CNS Drugs 21(8): 677–692.
2. Foley P (2000) The L-DOPA story revisited. Further surprises to be expected. J Neural Transm Suppl 60: 1–20.
3. Dunnett SB, Bjorklund A (1999) Prospects for new restorative and neuroprotective treatments in Parkinson's disease. Nature 399 (6738S): A32–A39.
4. LeWitt PA, Nyholm D (2004) New developments in levodopa therapy. Neurology 62 (S1): S9–S16.
5. Carta M, Carlsson T, Kirik D, Björklund A (2007) Dopamine released from 5-HT terminals is the cause of L-DOPA-induced dyskinesia in parkinsonian rats. Brain 130(7): 1819–1833.
6. Cenci MA (2007) Dopamine dysregulation of movement control in L-DOPA-induced dyskinesia. Trend Neurosci 30(5): 236–243.
7. Fabbrini G, Brotchie JM, Grandas F, Nomoto M, Goetz CG (2007) Levodopa-induced dyskinesias. Mov Disord 22(10): 1379–1389.
8. Boll MC, Sotelo J, Otero E, Alcaraz-Zubeldia M, Rios C (1999) Reduced ferroxidase activity in the cerebrospinal fluid from patients with Parkinson's disease. Neurosci Lett 265: 155–158.
9. Dexter DT, Carayon A, Vidailhet M, Ruberg M, Agid F, et al. (1990) Decreased ferritin levels in brain in Parkinson's disease. J Neurochem 55: 16–20.
10. Chang YZ, Ke Y, Du JR, Halpern GM, Ho KP, et al. (2006) Increased DMT1 expression might be associated with the neurotoxicity of L-DOPA. Mol Pharmacol 69(3): 968–974.
11. Ho KP, Li L, Zhao L, Qian ZM (2003) Genistein protects primary cortical neurons from iron-induced lipid peroxidation. Mol Cell Biochem 247(1–2): 219–222.
12. Qian ZM, Liao QK, To Y, Ke Y, Tsoi YK, et al. (2000) Transferrin-bound and transferrin-free iron uptake by the cultured brain astrocytes. Cell Mol Biol 46(3): 541–548.
13. Qian ZM, To Y, Feng YM (1999) Transferrin receptor on the plasma membrane of cultured rat astrocytes. Exp Brain Res 129(3): 473–476.
14. He W, Qian ZM, Zhu L, Christopher Q, Du F, et al. (2008) Ginkgolides mimic the effects of hypoxic preconditioning to protect C6 cells against ischemic injury by up-regulation of HIF-1α and EPO. Int J Biochem Mol Biol 40(4): 651–662.
15. Zhu L, Ke Y, Wu X, Yang L, Lu Y, Qian ZM (2008) Ginkgolides protect PC12 cells against hypoxia-induced injury by p42/p44 MAPK pathway-dependent upregulation of HIF-1α expression and HIF-1DNA-binding activity. J Cell Biochem 103: 564–575.
16. Zhu L, Lai Z, Ya K, Fang D, Ho YW, et al. (2008) Correlation between the expression of divalent metal transporter 1 and the content of hypoxia-inducible factor-1 in hypoxic HepG2 cells. J Cell Mol Med 12(2): 569–579.
17. Ke Y, Chang YZ, Duan XL, Du JR, Zhu L, et al. (2005) Iron-independent and Age-dependent Expression of the Two mRNA Isoforms of divalent metal transporter 1 in Different Brain Regions of Rats. Neurobiol Aging 26(5): 739–748.

18. Chang YZ, Qian ZM, Wang K, Zhu L, Yang XD, et al. (2005) Effects of development and iron status on ceruloplasmin expression in rat brain. J Cell Physiol 204(2): 623–631.
19. Qian ZM, Morgan EH (1992) Changes in the uptake of transferrin-free and transferrin-bound iron during reticulocyte maturation in vivo and in vitro. Biochim Biophys Acta 1135: 35–43.
20. Olanow CW, Obeso JA, Stocchi F (2006) Drug insight: Continuous dopaminergic stimulation in the treatment of Parkinson's disease. Nat Clin Pract Neurol 2(7): 382–392.
21. Zesiewicz TA, Sullivan KL, Hauser RA (2007) Levodopa-induced dyskinesia in Parkinson's disease: epidemiology, etiology, and treatment. Curr Neurol Neurosci Rep 7(4): 302–310.
22. Touret N, Furuya W, Forbes J, Gros P, Grinstein S (2003) Dynamic traffic through the recycling compartment couples the metal transporter Nramp2 (DMT1) with the transferrin receptor. J Biol Chem 278: 25548–25557.
23. Tanaka J, Toku K, Zhang B, Ishihara K, Sakanaka M, et al. (1999) Astrocytes prevent neuronal death induced by reactive oxygen and nitrogen species. Glia 28(2): 85–96.
24. Dringen R, Gutterer JM, Hirrlinger J (2000) Glutathione metabolism in brain metabolic interaction between astrocytes and neurons in the defense against reactive oxygen species. Eur J Biochem 267(16): 4912–4916.
25. Dhandapani KM, Hadman M, De Sevilla L, Wade MF, Mahesh VB, et al. (2003) Astrocyte protection of neurons: role of transforming growth factor-beta signaling via a c-Jun-AP-1 protective pathway. J Biol Chem 278(44): 43329–43339.
26. Mena MA, Casarejos MJ, Carazo A, Paino CL, García de Yébenes J (1996) Glia conditioned medium protects fetal rat midbrain neurones in culture from L-DOPA toxicity. Neuroreport 7(2): 441–445.
27. Fleming MD, Trenor CC 3rd, Su MA, Foernzler D, Beier DR, et al. (1997) Microcytic anemia mice have a mutation in Nramp2, a candidate iron transporter gene. Nature Genet 27: 383–386.
28. Gunshin H, Mackenzie B, Berger UV, Gunshin Y, Romero MF, et al. (1997) Cloning and characterization of a mammalian proton coupled metal-ion transporter. Nature 388: 482–488.
29. Tandy S, Williams M, Leggett A, Lopez-Jimenez M, Dedes M, et al. (2000) Nramp2 expression is associated with pH-dependent iron uptake across the apical membrane of human intestinal Caco-2 cells. J Biol Chem 275: 1023–1029.
30. Mackenzie B, Takanaga H, Hubert N, Rolfs A, Hediger MA (2007) Functional properties of multiple isoforms of human divalent metal-ion transporter 1 (DMT1). Biochem J 403(1): 59–69.
31. Burdo JR, Menzies SL, Simpson IA, Garrick LM, Garrick MD, et al. (2001) Distribution of divalent metal transporter 1 and metal transport protein 1 in the normal and Belgrade rat. J Neurosci Res 66: 1198–1207.
32. Picard V, Govoni G, Jabado N, Gros P (2000) Nramp 2 (DCT1/DMT1) expressed at the plasma membrane transports iron and other divalent cations into a calceinaccessible cytoplasmic pool. J Biol Chem 275: 35738–35745.